A Study on the Solid–Solid Phase Transitions of (*E*)- and (*Z*)-9-(Bicyclo[4.2.1]nonan-9-ylidene)bicyclo[4.2.1]nonane and Some Related Compounds. Assignment of the Configuration to the Product of Monoepoxidation of (*E*)-9-(Bicyclo[4.2.1]non-3-en-9-ylidene)bicyclo-[4.2.1]non-3-ene by ^{1}H Nuclear Magnetic Resonance Spectroscopy using the Shift Reagent Eu(fod)$_3$

Mercedes Marcos, Enrique Meléndez,* and José Luis Serrano
Departamento de Química Orgánica, Facultad de Ciencias, Universidad de Zaragoza, Zaragoza, Spain
Pelayo Camps,*,† Marta Figueredo, and Carlos Jaime
Departamento de Química Orgánica, Facultad de Ciencias, Universidad Autónoma de Barcelona, Bellaterra, Barcelona, Spain

The solid–solid phase transitions of (*E*)- and (*Z*)-9-(bicyclo[4.2.1]non-3-en-9-ylidene)bicyclo-[4.2.1]non-3-ene (1) and (2), (*E*)- and (*Z*)-9-(bicyclo[4.2.1]nonan-9-ylidene)bicyclo[4.2.1]nonane (3) and (4), (1*R*,1″*R*,6*S*,6″*S*,9*r*,9″*r*)- and (1*R*,1″*R*,6*S*,6″*S*,9*r*,9″*s*)-dispiro(bicyclo[4.2.1]nonane-9,2′-oxirane-3′,9″-bicyclo[4.2.1]nonane) (5a) and (6), and (1*R*,1″*R*,6*S*,6″*S*, 9*s*,9″*s*)- and (1*R*,1″*R*,-6*S*,6″*S*,9*r*,9″*s*)-dispiro(bicyclo[4.2.1]non-3-ene-9,2′-oxirane-3′,9″-bicyclo[4.2.1]non-3″-ene) (7a) and (8) are studied by differential scanning calorimetry. In general, the *syn*-compounds, (1), (3), (5a), and (7a) show higher m.p.s and exhibit plasticity over a larger range of temperatures than *anti*-compounds (2), (4), (6), and (8). The intracyclic double bond is a negative factor for plasticity in these compounds. The unit-cell dimensions of alkene (4) and epoxide (7a) have been determined by *X*-ray diffraction. The configuration of epoxide (7a) has been established through the comparison of its 200 MHz ^{1}H n.m.r. spectrum with those of the epoxide (8) and the model compounds *syn*- (9) and *anti*-bicyclo[4.2.1]non-3-en-9-ol (10). Also, the assigned configuration of epoxide (7a) has been confirmed through the analysis of its ^{1}H n.m.r. spectrum in the presence of known amounts of the shift reagent Eu(fod)$_3$.

In a previous publication [1] we described the preparation of (*E*)- and (*Z*)-9-(bicyclo[4.2.1]non-3-en-9-ylidene)bicyclo[4.2.1]-non-3-ene (1) and (2), (*E*)- and (*Z*)-9-(bicyclo[4.2.1]nonan-9-ylidene)bicyclo[4.2.1]nonane (3) and (4), and (1*R*,1″*R*,6*S*,-6″*S*,9*r*,9″*r*)- and (1*R*,1″*R*,6*S*,6″*S*,9*r*,9″*s*)-dispiro(bicyclo-[4.2.1]nonane-9,2′-oxirane-3′,9″-bicyclo[4.2.1]nonane) (5a) and (6), respectively, in connection with a study of the Ti^0 reduction of bicyclo[4.2.1]non-3-en-9-one. At that time, the configuration for the product of epoxidation of alkene (3) was not known. However, assuming that epoxidation takes place at the less hindered carbon–carbon double bond *re*-face, (5a) was tentatively assigned as being the product.

The m.p.s of some of these compounds could not be determined by the usual methods. Detailed observation of the phenomenon by optical microscopy showed that compounds (3), (4), (5a), and (6) have, in the proximity of their m.p.s, a mosaic texture similar to that observed in the S_G and S_B mesophase of some mesogenic compounds.[2] A very rapid solid–solid phase transition for compounds (4) (71 °C) and (5a) (75 °C) was also easily detected with polarized light showing a pseudoisotropic texture. These observations and the structural similarity of the semimolecule of these compounds to some compounds showing solid-state transitions [3,4] suggested that these compounds could present plastic crystalline behaviour.

This led us to undertake a more complete study of these properties and to establish the configuration of (5a), as described later, through the preparation of the new compounds (1*R*,1″*R*,6*S*,6″*S*,9*s*,9″*s*)- and (1*R*,1″*R*,6*S*,6″*S*,9*r*,9″*s*)-dispiro(bicyclo[4.2.1]non-3-ene-9,2′-oxirane-3′,9″-bicyclo-[4.2.1]non-3″-ene) (7a) and (8), by selective epoxidation of (1) and (2), respectively. Compound (7a) showed similar optical properties to those observed for compounds (3), (4)' (5a), and (6).

† *Present address:* Departamento de Química Orgánica, Facultad de Químicas de San Sebastián, Universidad del País Vasco, San Sebastián, Spain.

Results and Discussion

Differential Scanning Calorimetric Studies.—The thermal and thermodynamic properties of all of these compounds are collected in Table 1. As can be seen from Table 1, compounds (3), (4), and (5a)—(7a) show solid–solid phase transitions. Although the entropy of this transition in compound (6) is very small, its macroscopic and optical properties and plastic crystalline behaviour are similar to those observed in compounds (3), (4), (5a), and (7a). The small values for the entropies of fusion of these compounds confirm the formation of plastic phases. However, with the exception of compound (6), these values are higher than the arbitrary limit given by Timmermans [5] for plastic crystals, $\Delta S_m \leqslant 20$ J K^{-1} mol^{-1}. The difference is specially noticeable for compounds (4) and (5a), which also show the highest entropies for the solid–solid phase transitions. Compounds (2) and (8), which do not exhibit plastic crystalline behaviour, have higher entropies of fusion than those observed for compounds (3), (4), (5), (5a), (6), and (7a). Compound (1) shows some anomalies near its m.p. and has a low entropy of fusion. However, no solid–solid phase transition was observed in the range of temperature studied.

In general, the *syn*-compounds [(1), (3), (5a), and (7a)] show higher m.p.s and exhibit plasticity over a larger range of temperatures than the *anti*-ones [(2), (4), (6), and (8)]. Better molecular arrangements and greater intermolecular interaction in the crystals of the *syn*-compounds would seem to account for this phenomenon. In the compounds under study, the intracyclic double bond is a negative factor for plasticity and only one of the compounds having this type of bonding, (7a), exhibits plastic crystalline behaviour over a short range of temperature.

Table 1. Thermal and thermodynamic data for compounds (1)—(4), (5a), (6), (7a), and (8)

Compound	Transition	T/K	ΔH/kJ mol^{-1}	ΔS/J K^{-1} mol^{-1}
(1)	Fusion	441.70 ± 1.0 [a]	9.10 ± 0.5 [a]	20.60 ± 1.2 [a]
(2)	Fusion	440.75 ± 0.1	27.96 ± 0.11	64.33 ± 0.6
(3)	T_1 [b]	224.75 ± 0.1	2.68 ± 0.03	11.92 ± 0.1
	Fusion	412.40 ± 0.1	9.32 ± 0.04	22.61 ± 0.2
(4)	T_1 [b]	344.30 ± 0.1	10.12 ± 0.04	29.39 ± 0.2
	Fusion	393.30 ± 0.1	11.04 ± 0.05	28.05 ± 0.3
(5a)	T_1 [b]	348.45 ± 0.1	9.74 ± 0.03	27.92 ± 0.3
	Fusion	444.05 ± 0.1	13.13 ± 0.03	29.55 ± 0.3
(6)	T_1 [b]	274.90 ± 0.1	0.72 ± 0.01	2.59 ± 0.05
	Fusion	342.50 ± 0.1	6.35 ± 0.02	18.52 ± 0.1
(7a)	T_1 [b]	354.25 ± 0.1	5.98 ± 0.02	16.85 ± 0.1
	Fusion	373.75 ± 0.1	8.19 ± 0.02	21.86 ± 0.1
(8)	Fusion	333.85 ± 0.1	14.92 ± 0.06	44.60 ± 0.3

[a] The less accurate values in this case are due to the small quantity of product available. [b] Solid–solid phase transition.

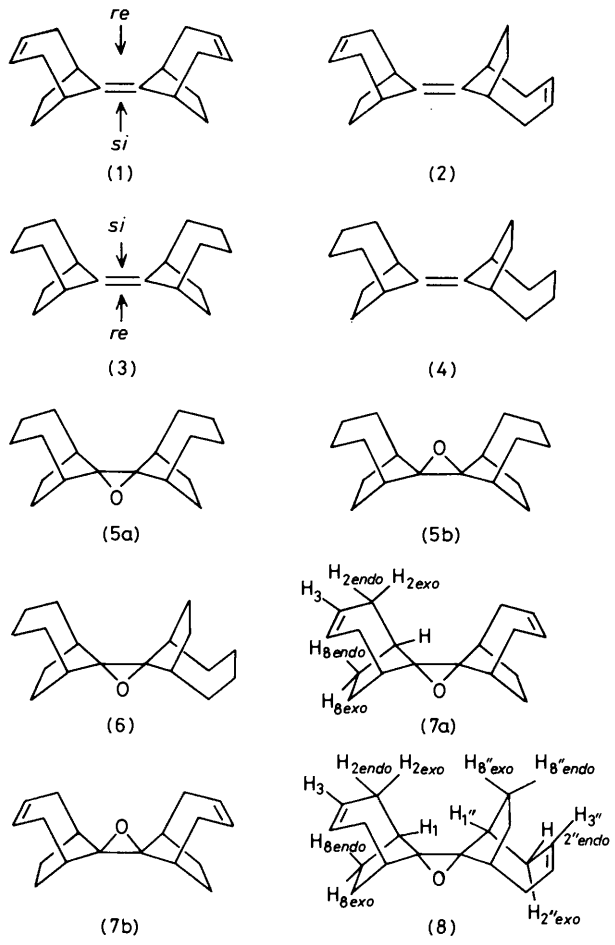

Crystallographic Studies.—Preliminary observation of the molecular dimensions of these compounds obtained from modified MM2-minimized structures [6] (Table 2) shows that none of them have the typical globular form generally observed for the compounds exhibiting plastic crystalline behaviour. All of them have a well defined predominant axis, although the relative length is slightly greater for the *anti*-compounds than for the *syn*-ones.

The unit cell dimensions in the plastic phases of compounds (4) and (7a) were determined by *X*-ray diffraction. Compound (4) (*T* 373 K; 24 h exposure) shows a cubic unit cell with a constant value a = 11.83 Å, which contains four molecules. In this compound, the semimolecule joins the plastic crystal characteristics. Thus, each unit cell contains eight pattern units. Compound (7a) (*T* 365 K; 24 h exposure) shows a tetragonal unit cell with constant values $a = b$ = 7.40 Å and c = 5.89 Å, which contains only one molecule. These values indicate a more compact structure for the molecules of (7a) than those of (4): V[unit cell (4)] = 1 640 Å^3, V[molecule (4)] = 410 Å^3, V[unit cell (7a)] = 322 Å^3, V[molecule (7a)] = 322 Å^3. This fact is in accord with the expected better molecular arrangement and greater molecular interaction in the crystals of the *syn*-compounds.

Table 2. Molecular dimensions including van der Waals' radii for compounds (1)—(4), (5a), (6), (7a), and (8), as calculated by 'modified MM2' [a]

	Å			Relative values		
Compd.	length	width	height	length	width	height
(1)	10.36	8.06	7.88	1.31	1.02	1
(2)	11.42	8.72	7.81	1.46	1.05	1
(3)	10.37	8.21	7.85	1.32	1.05	1
(4)	11.05	8.42	7.80	1.42	1.08	1
(5a)	10.61	7.87	8.37	1.27	0.94	1
(6)	11.54	8.09	7.90	1.46	1.02	1
(7a)	10.61	8.12	7.97	1.33	1.02	1
(8)	11.49	7.97	7.86	1.46	1.01	1

[a] The terms length, width, and height refer to maximum values of the molecular orientation given.

Assignment of the Configuration to the Epoxides obtained from Compounds (1) *and* (3).—As we have indicated elsewhere,[1] epoxidation of alkene (3) can give two epoxides of the same point group (5a and b). However, only one was obtained whose configuration could not be established through the analysis of its 200 and 60 MHz ^{1}H n.m.r. spectra in the presence of different quantities of the shift reagent tris-(1,1,1,2,2,3,3-heptafluoro-7,7-dimethyloctane-4,6-dionato)europium Eu(fod)$_3$, due to the small chemical shift difference between all the methylene protons of this compound.

In order to solve this problem, we have selectively epoxidized the tetrasubstituted carbon–carbon double bond of compounds (1) and (2). Reaction of (1) with a small molar deficit of *m*-chloroperbenzoic acid in methylene chloride afforded only one unsaturated epoxide, (7a) or (7b) (94%), which on hydrogenation (10% Pd–C; H_2; 1 atm; ethyl acetate) gave a saturated epoxide, identical (g.l.c.) with the only epoxide obtained by epoxidation of (3). Consequently, they must have the same configuration. In a similar manner,

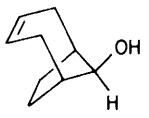

(9)

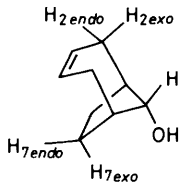

(10)

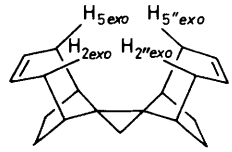

(11)

(12)

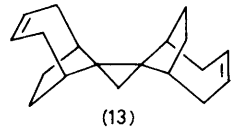

(13)

Table 3. Chemical shifts for some significative protons of alcohols (9) and (10) and epoxides (7a or b) and (8)

Compound	H2(5)*exo*	H2″(5″)*exo*	H7(8)*exo*	H7″(8″)*exo*
(9)	2.40		1.80	
(10)	2.18		2.12	
(7a) or (7b)	2.40		2.10	
(8)	2.36	2.1	1.82	2.1

epoxidation of alkene (2) gave an unsaturated epoxide (8) in 92% yield, which on hydrogenation, as expected, gave the saturated epoxide (6).

The comparison of the 200 MHz ^{1}H n.m.r. spectrum of epoxide (7a or b) with those of (8) and the model compounds *syn*-bicyclo[4.2.1]non-3-en-9-ol [7] (9), and *anti*-bicyclo[4.2.1]-non-3-en-9-ol [7] (10) (Table 3) points to the configuration shown in (7a) for the product of monoepoxidation of alkene (1), a fact which is in agreement with the expected epoxidation at the less hindered carbon–carbon double bond *si*-face.

In the following discussion we assume the cycloheptene rings of alcohols (9) and (10) and epoxides (7a or b) and (8) to have the chair conformation. Molecular mechanics calculations (Allinger's latest empirical force-field program MM2) [8] showed the clear preference of bicyclo[4.2.1]non-3-ene to have a chair cycloheptene ring. The torsional-energy surface corresponding to the equilibrium chair–boat shows a global energy minimum for the chair conformer (ΔH_f 8.32 kJ mol^{-1}) and a flat region (23.16 kJ mol^{-1} higher than chair) for the boat conformer. The surface also contains two twisted valleys connecting both the key points and reflecting the high strain energy that a symmetric intermediate with a planar cycloheptene ring should have. Therefore, it seems reasonable to assume chair cycloheptene rings for the compounds under study. On this hypothesis, the dihedral angle H2(5)*endo*-C–C–H3(4) in all these compounds should be near 0°, while H2(5)-*exo*-C–C–H3(4) should be near 90°. According to the Karplus equation a larger $J_{H2(5)endo-H3(4)}$ value is to be expected. This fact helped us in assigning the absorptions of the H2(5)*exo* and H2(5)*endo* protons of these compounds. Moreover, the effect of the hydroxy-function on the chemical shift of the H7(8)*exo* protons of the alcohols (9) and (10) of known configuration simplified the assignment of the H7(8)*exo* and H7(8)*endo* protons of the epoxides (7a or b) and (8).

As can be seen from Table 3, the chemical shift for the H7(8)*exo* protons of (10) is 0.32 p.p.m. downfield with respect to the corresponding absorption in (9), due to the proximity of the hydroxy-group.[9] For the same reason, the chemical shift for the H2(5)*exo* protons of (9) is 0.22 p.p.m. downfield with respect to the corresponding absorption in (10). In epoxide (8), one part of the molecule resembles alcohol (10), while the other resembles alcohol (9). Accordingly, two absorptions differing by *ca.* 0.3 p.p.m. for the H7(8)*exo* and H7″(8″)*exo* protons, and two absorptions differing by *ca.* 0.3 p.p.m. for the H2(5)*exo* and H2″(5″)*exo* protons, are observed. In epoxide (7a), both parts of the molecule resemble alcohol (10), while in (7b) they resemble alcohol (9). In fact, the chemical shift for the H7(8)*exo* protons agrees for (7a), but the chemical shift for the H2(5)*exo* protons is *ca.* 0.2 p.p.m. downfield with respect to the expected value. However, this downfield shifting might be due to a van der Waals' effect.[9]

Since molecular mechanics calculations give intramolecular H · · · H non-bonded distances *ca.* 0.1 Å larger than real ones,[10] we undertook calculations on the model compounds (11)—(13) * using a ' modified MM2 ' program [6] which gives values much closer to the experimental ones than does MM2. A van der Waals' energy of 2.49 kJ mol^{-1} between the pairs of protons H2*exo*–H2″*exo* and H5*exo*–H5″*exo* of compound (11) and a distance of 1.97 Å between these pairs of protons were obtained. Since the molecular geometry of epoxide (7a) must be very close to that of compound (11), a downfield shift of *ca.* 0.2 p.p.m. is to be expected for the H2(5)*exo* protons of (7a).[9] No similar situation was found for compounds (12) and (13).

To confirm the configuration of the product of epoxidation of alkene (1), we determined the Eu(fod)$_3$-induced chemical shifts (LICS) † at 0.39, 0.59, and 0.79 Eu(fod)$_3$: substrate molar ratios. Plots of the LICS for the different protons of (7a or b) *versus* the Eu(fod)$_3$: substrate molar ratio gave straight lines in all cases.

According to the equation of McConnell and Robertson,[11] $\Delta\delta_i = K(3\cos^2\varphi_i - 1)/r_i^3$, the LICS of a proton is a function of its distance to the lanthanide atom, r_i, and the co-ordination angle, φ_i (*i.e.* the angle formed by the line that joins the lanthanide atom and the proton under consideration and the principal axis of the complex). If we consider the complexes of (7a or b) with Eu(fod)$_3$, the europium atom must lie on average along the C_2 axis of symmetry of these epoxides, which must be the principal axis of the corresponding complexes.

On these grounds, and using the ' modified MM2 ' minimized structures for compounds (11) and (12) as models for (7a and b), we have calculated the r_i and φ_i values for the complexes of (7a and b) with Eu(fod)$_3$ at several oxygen–europium distances (from 2.0 to 4.0 Å).[11]

An acceptable correlation of LICS with $(3\cos^2\varphi_i - 1)/r_i^3$ was obtained for (7a) at an oxygen–europium distance of 3.5 Å, (Figure) while no such correlation was obtained for (7b), thus

* The C_{sp^2}–C_{sp^3}–C_{sp^3}–$C_{cyclopropane}$ torsional parameter was lacking but provisionally set equal to that for C_{sp^2}–C_{sp^3}–C_{sp^3}–C_{sp^3}.

† The ^{1}H n.m.r. spectra in the presence of Eu(fod)$_3$ were taken at 60 MHz, because the LICS at 200 MHz were very small, probably due to the highly dilute solutions in this case. However, the initial δ values used to calculate the LICS were obtained from the 200 MHz spectrum. Evidence proving the correctness of this replacement was obtained by plotting the LICS for the different protons of (7a or b), obtained from the 60 MHz spectra taking the spectrum in the presence of 0.39 equiv. of Eu(fod)$_3$ as starting point, *versus* the increment in the Eu(fod)$_3$: substrate molar ratio. Straight lines of the same slope as those obtained when the LICS were calculated from the initial δ values (200 MHz spectrum) were obtained.

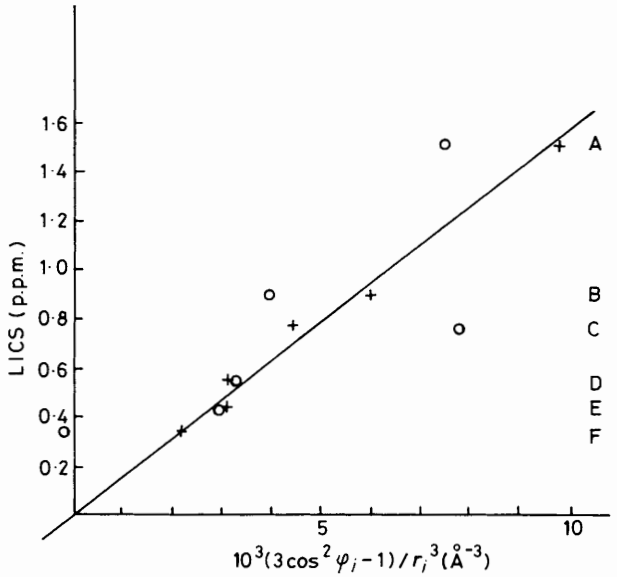

Figure. Plot of the LICS (p.p.m.) at 0.59 Eu(fod)$_3$: substrate molar ratio *vs.* $(3\cos^2\varphi_i - 1)/r_i^3$ (Å^{-3}), for the protons of (7a) (+) and (7b) (O), the europium atom being an average of 3.5 Å from the oxirane oxygen atom along the C_2 axis of symmetry. A, H1(6); B, H7(8)*exo*; C, H2(5)*exo*; D, H7(8)*endo*; E, H2(5)*endo*; F, H3(4)

confirming the configuration of the product of epoxidation of (1) as (7a). Consequently, the configuration of the product of epoxidation of alkene (3) must be that shown for (5a).

Experimental

I.r. spectra were recorded on a Perkin-Elmer Infracord 720 spectrometer, mass spectra on a Hewlett-Packard 5930 A spectrometer, 60 MHz ^{1}H n.m.r. spectra on a Perkin-Elmer R-12 spectrometer, and 200 MHz spectra on a Varian XL 200 spectrometer. Chemical shifts are referred to internal tetramethylsilane. G.l.c. analysis were carried out on a Perkin-Elmer Sigma-1 chromatograph. Elemental analyses were performed in the Analytical Section, Instituto de Química Bio-orgánica, Barcelona.

The purity of samples was at least 99.9% as determined by g.l.c. analysis and confirmed by differential scanning calorimetry.[12]

Microscopic data were obtained by using a Reichert-Thermovar HT1, B11, polarizing microscope equipped with a heating stage. The thermal and thermodynamic data were obtained by using a Perkin-Elmer DSC-2 apparatus provided with an integrator. The samples in sealed aluminium pans were analysed at temperatures ranging from 150 K to fusion. The energy was calibrated by using standard samples of pure indium (the value 28.42 J K^{-1} mol^{-1} was used for its enthalpy of fusion); the scale of temperature was calibrated by using standard samples of tin (T_{fus} 505.06 K), indium (T_{fus} 429.78 K), and water (T_{fus} 273.10 K). The transition temperatures and thermodynamic data were determined using a heating rate of 0.25 K min^{-1} and corroborated using a heating rate of 4.00 K min^{-1}. Except for compound (1) (only one sample), three different samples for each compound were used and two runs per sample were carried out.

The diffraction experiments from powder diagrams were performed using a Guinier camera (Co-K_{α_1} radiation was used) equipped with a heating stage.

Calculations were carried out at the Computing Center, Hokkaido University, Sapporo, on a HITAC M-200H system.

Epoxidation of (1). (1R,1″R,6S,6″S,9s,9″s)-*Dispiro*(*bicyclo*[4.2.1]*non*-3-*ene*-9,2′-*oxirane*-3′,9″-*bicyclo*[4.2.1]*non*-3″-*ene*) (7a).—To a cold solution of (1) (30 mg, 0.125 mmol) in CH_2Cl_2 (3 ml), a cold solution of 85% *m*-chloroperbenzoic acid (25 mg, 0.123 mmol) was added and the mixture was allowed to react at 0 °C for 2 h. The solution was filtered through Al_2O_3 (3 g) giving rise by evaporation of the solvent to (7a) (30 mg, 94%) as a solid, pure by g.l.c., which was sublimed at 90 °C and 15 Torr, m.p. 101 °C, i.r. spectrum not definitive, δ ($CDCl_3$; 200 MHz) 1.48 (4 H, m, H7*endo* and H8*endo*), 2.0—2.3 (12 H, complex, H1, H2*endo*, H5*endo*, H6, H7*exo*, and H8*exo*), 2.40 (4 H, m, H2*exo* and H5*exo*), 5.62 (4 H, m, H3 and H4), on irradiation at δ 2.1, the absorption at δ 5.62 became a singlet, on irradiation at δ 2.40 the absorption at δ 5.62 remained unchanged, *m/e* 257(*M* + 1, 1%), 256(*M*, 6), 136(28), 121(37), 120(28), 119(28), 105(28), 93(36), 92(46), and 91(100) (Found: C, 84.3; H, 9.55. $C_{18}H_{24}O$ requires C, 84.3; H, 9.45%).

Epoxidation of (2). (1R,1″R,6S,6″S,9r,9″s)-*Dispiro*(*bicyclo*[4.2.1]*non*-3-*ene*-9,2′-*oxirane*-3′,9″-*bicyclo*[4.2.1]*non*-3″-*ene*) (8).—This was prepared as described for (7a). From (2) (150 mg, 0.625 mmol), (8) (92%, 147 mg), pure by g.l.c., was obtained and sublimed at 80 °C and 15 Torr, m.p. 61 °C, i.r. spectrum not definitive, δ ($CDCl_3$; 200 MHz) 1.46—1.66 (4 H, complex, H7*endo*, H7″*endo*, H8*endo*, and H8″*endo*), 1.78—1.86 (2 H, m, H7*exo* and H8*exo*), 2.00—2.26 (12 H, complex, H1, H2*endo*, H5*endo*, H6, H1″, H2″*endo*, H2″*exo*, H5″*endo*, H5″*exo*, H6″, H7″*exo*, and H8″*exo*), 2.36 (2 H, m, H2*exo* and H5*exo*), and 5.58 (4 H, m, H3, H4, H3″, and H4″), on irradiation at δ 2.36 the absorption at δ 5.58 remained unchanged, *m/e* 257(*M* + 1, 0.1%), 256(*M*, 0.6), 131(10), 129(10), 121(15), 120(36), 119(25), 117(20), 105(25), 95(20), 93(33), 92(44), and 91(100) (Found: C, 84.3; H, 9.5%).

Acknowledgements

We thank Drs. A. M. Levelut and L. Liebert, Université de Paris-Sud, Orsay, for carrying out the *X*-ray diffraction studies and Professor E. Ōsawa, Hokkaido University, Sapporo, for facilities to carry out the theoretical calculations.

References

1 R. Amposta, P. Camps, M. Figueredo, C. Jaime, and A. Virgili, *An. Quim., Ser. C*, 1981, **77**, 267.
2 D. Demus and L. Richter, 'Textures of Liquid Crystals,' Verlag Chemie, Weinheim, 1978, pp. 148 and 174.
3 K. Bystrom, *J. Chem. Soc., Faraday Trans. 1*, 1980, **76**, 1986.
4 P. Cuvalier and J. Billard, *Mol. Cryst. Liq. Cryst.*, 1980, **64**, 33.
5 J. Timmermans, *J. Chim. Phys.*, 1938, **35**, 331.
6 C. Jaime and E. Ōsawa, *Tetrahedron*, 1983, **39**, 2769.
7 R. S. Brown and R. W. Marcinko, *J. Am. Chem. Soc.*, 1977, **99**, 6500.
8 (*a*) N. L. Allinger, *J. Am. Chem. Soc.*, 1977, **99**, 8127; (*b*) N. L. Allinger and Y. H. Yuh, Quantum Chemistry Program Exchange, 1981, vol. 13, p. 395.
9 L. M. Jackman and S. Sternhell, 'Applications of Nuclear Magnetic Resonance Spectroscopy in Organic Chemistry,' Pergamon, Oxford, 1969, 2nd. edn., pp. 78—79.
10 E. Ōsawa and H. Musso, *Top. Stereochem.*, 1982, **13**, 117.
11 R. Ammon and R. D. Fischer, *Angew. Chem., Int. Ed. Engl.*, 1972, **11**, 675.
12 H. Staub and W. Pemon, *Anal. Chem.*, 1974, **46**, 128.

Received 21*st December* 1982; *Paper* 2/2139